

Published in final edited form as:

Mucosal Immunol. 2013 July ; 6(4): 678–691. doi:10.1038/mi.2012.106.

Migratory properties of pulmonary dendritic cells are determined by their developmental lineage

H Nakano¹, JE Burgents¹, K Nakano¹, GS Whitehead¹, C Cheong², CD Bortner³, and DN Cook¹

¹Laboratory of Respiratory Biology, National Institute of Environmental Health Sciences, NIH, Research Triangle Park, North Carolina, USA

²Laboratory of Cellular Physiology and Immunology and Chris Browne Center for Immunology and Immune Diseases, The Rockefeller University, New York, New York, USA

³Laboratory of Signal Transduction, Division of Intramural Research, National Institute of Environmental Health Sciences, NIH, Research Triangle Park, North Carolina, USA

Abstract

The chemokine receptor, CCR7, directs the migration of dendritic cells (DCs) from peripheral tissue to draining lymph nodes (LNs). However, it is unknown whether all pulmonary DCs possess migratory potential. Using novel *Ccr7^{gfp}* reporter mice, we found that *Ccr7* is expressed in CD103⁺ and a CD14^{med/lo} subset of CD11b^{hi} classical (c) DCs but not in monocyte-derived (mo) DCs, including Ly-6C^{hi}CD11b^{hi} inflammatory DCs and CD14^{hi}CD11b^{hi} DCs. Consequently, cDCs migrated to lung-draining LNs but moDCs did not. Mice lacking the chemokine receptor, CCR2, also lacked inflammatory DCs in the lung after lipopolysaccharide inhalation but retained normal levels of migratory DCs. Conversely, the lungs of *fms*-like tyrosine kinase 3 ligand (*Flt3L*)-deficient mice lacked cDCs but retained moDCs, which were functionally mature but did not express *Ccr7* and were uniformly non-migratory. Thus, the migratory properties of pulmonary DCs are determined by their developmental lineage.

INTRODUCTION

Dendritic cells (DCs) initiate adaptive immune responses by processing antigens and presenting them to T cells.¹ In the lung, the actions of DCs determine whether inhaled antigens elicit effector or tolerogenic immune responses.² DC migration from the lung to draining lymph nodes (LNs) proceeds at low levels during steady-state conditions, but the rate and volume of that migration is increased following exposure to pro-inflammatory stimuli.^{3,4} However, some antigen-bearing DCs remain in the lung for prolonged periods,^{5–7} and selective depletion of DCs during the challenge phase of murine models of asthma abrogates allergic responses.^{8,9} These data suggest that DC retention in the lung might be important to activate memory T cells arriving in the lung. It is unknown, however, whether all DCs that are exposed to appropriate stimuli have the capacity to migrate to draining LNs. One possibility is that some lung DCs reside in an anatomical position that shields them from stimuli that would otherwise promote migration. Alternatively, DCs might become

© 2012 Society for Mucosal Immunology

Correspondence: DN Cook (cookd@niehs.nih.gov).

SUPPLEMENTARY MATERIAL is linked to the online version of the paper at <http://www.nature.com/mi>

DISCLOSURE

The authors declared no conflict of interest.

migratory on a stochastic basis that ensures an appropriate distribution of DCs in the lung and draining LNs. A third possibility is that some DCs lack the capacity for migration.

Recent studies have shown that pulmonary DCs are not homogeneous but are comprised of multiple subsets that can be distinguished phenotypically by their display levels of various cell surface markers. As in other non-lymphoid tissues, DCs in the lung are comprised of two major classical cDC subsets: CD11c^{high}(^{hi})CD11b^{hi}CD103⁻ DCs and CD11c^{hi}CD11b^{low}(^{lo})CD103⁺ DCs,¹⁰ often referred to as CD11b^{hi} and CD103⁺ DCs, respectively. CD103⁺ DCs are tightly associated with the respiratory epithelium and extend processes into the lumen of the airway.¹⁰ These cells represent the major DC subset in the lung for cross-presenting antigens to CD8⁺ T cells,¹¹ promoting viral clearance¹² and directing T helper type 2 (Th2) responses to inhaled allergens.¹³ CD11b^{hi} DCs reside beneath the epithelium and can produce large amounts of chemokines.¹⁴ In addition to CD11b^{hi} DCs that are present in the lung during homeostasis, Ly-6C⁺CD11c^{int}CD11b^{hi} monocyte-derived DCs (moDCs) are rapidly recruited to the lung during inflammation.¹⁵ moDCs also display high levels of CD14, which distinguishes them from CD11b^{hi} cDCs.¹⁶

The migration of DCs to draining LNs is guided by interactions between the chemokine receptor, CCR7, and its ligands, CCL19 and CCL21, which are produced in the lymphatic vessels and in T-cell areas of LNs.¹⁷⁻¹⁹ Many CD103⁺ DCs display CCR7 and are dependent on this receptor for their migration to lung-draining mediastinal (m)LNs.²⁰ Consequently, CD103⁺ DCs are virtually absent in mLNs of *Ccr7*^{-/-} mice. However, CD11b^{hi} DCs can be found in mLNs of these mice, albeit at reduced levels compared with those of wild-type mice,^{13,20} suggesting that CD11b^{hi} DCs can gain access to mLNs by both CCR7-dependent and -independent pathways. Other studies have confirmed that under some circumstances, CD11b^{hi} DCs can migrate from the lung to mLNs,^{21,22} but it is unclear whether all CD11b^{hi} DCs have this potential.

DCs are derived from monocytes and the common DC precursor (CDP).^{23,24} The latter can differentiate into either plasmacytoid DCs or pre-DCs^{25,26}. Recent studies have suggested that CD103⁺ DCs are derived exclusively from CDPs and pre-DCs via a developmental pathway dependent on interactions between fms-like tyrosine kinase 3 (FLT3) and its ligand (FLT3L).^{27,28} However, CD11b^{hi} DCs in mucosal tissue can develop from monocytes, which do not require FLT3 or FLT3L for their differentiation into DCs.²⁴ Blood-borne monocytes are comprised of two distinct populations, expressing high levels of the CCR2 and CX3CR1, respectively,²⁹ and both of these populations can give rise to lung DCs, even during homeostatic conditions.³⁰ Thus, the lung contains CDP-derived classical CD103⁺ and CD11b^{hi} DCs (cDCs), as well as CD11b^{hi} moDCs. Whether CD11b^{hi} DCs in the lung that arise from these alternative developmental pathways possess different migratory capacities and functions is unknown. Here, we report that in the lung, FLT3-dependent CD103⁺ cDCs and CD11b^{hi} cDCs are migratory, whereas moDCs are non-migratory. These differences have important implications with regard to the initiation of primary T-cell responses in mLNs and stimulation of secondary T-cell responses in the lung.

RESULTS

CD103⁺ DCs and a subpopulation of CD11b^{hi} DCs are migratory

DCs in the lung were identified as low-density CD11c⁺I-A⁺ autofluorescence^{lo} cells (see Supplementary Figure S1a online). Although alveolar macrophages are also CD11c⁺,^{31,32} their autofluorescence and display of Siglec-F distinguishes them from DCs (see Supplementary Figure S1b online).³³ Accordingly, we used autofluorescence to gate out macrophages from our analysis of pulmonary DCs. In mLNs, DCs were identified as CD11c⁺I-A⁺CD3^{lo}CD19^{lo} cells. We confirmed that CD11b^{hi} DCs and CD103⁺ DCs are the

major DC subsets in the lungs of untreated mice, with CD103⁺ DCs being slightly more abundant (Figure 1a). Under steady-state conditions, most DCs in lung-draining mLNs were CD11b^{hi}, with very few CD103⁺ DCs (Figure 1b), in agreement with previous reports.³

DC migration from the lung to mLNs is increased following inhalation of pro-inflammatory stimuli, such as lipopolysaccharide (LPS).³⁴ We found that the total number of CD11b^{hi} DCs in the lung increased markedly during the 24-h period after instillation of ovalbumin (OVA) mixed with LPS (OVA/LPS), whereas the number of CD103⁺ DCs decreased (Figure 1a), suggesting that some of the latter cells had migrated to mLNs. Analysis of mLNs revealed that both CD11b^{hi} DCs and CD103⁺ DCs were dramatically increased after OVA/LPS treatment (Figure 1b). The latter DC subset was increased 10-fold over the very low levels seen in mLNs of untreated mice.

Although DCs ferry antigen from peripheral tissue to draining LNs, some soluble proteins such as OVA can be carried rapidly in the lymph from the lung to mLNs, where they are taken up by mLN DCs.²⁰ Thus, in studies of lung DC migration, it is critically important to distinguish between antigen-bearing DCs arriving from the lung and mLN-resident DCs that acquire soluble antigens while in the LN. Previous studies have shown that inhaled carboxyfluorescein diacetate succinimidyl ester (CFSE) stains lung-resident DCs, thereby allowing these cells to be identified after their migration to mLNs.²⁰ However, instillation of CFSE causes airway inflammation,³⁵ which confounds studies of DC trafficking during homeostasis. For this reason, we tested the utility of an alternative fluorescent dye, PKH26 (PKH),³⁶ and found that it readily stained pulmonary DCs. No DCs in mLNs were stained by PKH by 4 h after PKH instillation, indicating that unlike OVA, PKH is not passively carried in the lymph to LNs. This allowed us to track the migration of PKH-stained pulmonary DCs to mLNs (Figure 1c and see Supplementary Figures S1c,d online). Moreover, PKH did not induce airway inflammation, whereas CFSE did (see Supplementary Figure S1e online). Based on these results, we concluded that PKH was an appropriate dye to study pulmonary DC migration.

Instillation of OVA/LPS into the airway markedly increased the number of PKH⁺ DCs in mLNs compared with the number seen under steady-state conditions (Figures 1c,d). The vast majority of these migratory DCs were CD103⁺, although some PKH⁺ CD11b^{hi} DCs were also seen, and their numbers were also significantly increased by OVA/LPS. Most PKH⁺ DCs of both subsets displayed high levels of major histocompatibility complex (MHC) class II in agreement with a previous report showing that migratory DCs are MHC class II^{hi}.⁵ However, we found that some PKH⁺ CD11b^{hi} DCs displayed moderate levels of this molecule (see Supplementary Figure S1f online). Taken together, these data suggest that CD103⁺ DCs are the major migratory DC subset in the lung, although a subpopulation of CD11b^{hi} DCs also possesses migratory activity.

CD11b^{hi} DC migration from the lung to mLNs is CCR7-dependent

CD103⁺ DCs are virtually absent in mLNs of *Ccr7*^{-/-} mice, although some CD11b^{hi} DCs can be found (Figure 1e).^{13,20} This indicates that some CD11b^{hi} DCs can gain access to mLNs by both CCR7-dependent and -independent pathways. To determine whether CD11b^{hi} DCs can migrate from the lung to mLNs in a CCR7-independent manner, we used PKH staining of DCs to analyze their migration in wild-type and *Ccr7*^{-/-} mice. In mLNs of wild-type mice, most migratory PKH⁺ DCs were CD103⁺, although some PKH⁺ CD11b^{hi} DCs were also seen. However, mLNs of *Ccr7*^{-/-} mice contained almost no PKH⁺ DCs of either subset (Figure 1f). Thus, migration of lung CD11b^{hi} DCs, as well as that of CD103⁺ DCs, is critically dependent on CCR7, suggesting that the CD11b^{hi} DCs present in mLNs of *Ccr7*^{-/-} mice are not emigrants from the lung but likely arise from blood-borne precursors.

CD103⁺ DCs and a minor population of CD11b^{hi} DCs in the lung express *Ccr7*

The relatively high migratory activity of CD103⁺ DCs suggested that they might express higher levels of *Ccr7* than do CD11b^{hi} DCs. To test this, we purified the two major lung DC subsets and prepared mRNA from them. CD103⁺ DCs expressed more *Ccr7* mRNA than did CD11b^{hi} DCs (Figure 2a). Instillation of LPS increased *Ccr7* expression in both the DC subsets but much more strongly in CD103⁺ DCs. This higher level of *Ccr7* mRNA in CD103⁺ DCs might have been due to a larger proportion of *Ccr7*-expressing cells or to more *Ccr7* expression on a per cell basis. To distinguish between these possibilities, we attempted to estimate CCR7 display levels on individual cells by flow cytometry. Antibodies to CCR7 bound to this receptor on lung DCs and bone marrow-derived DCs (BMDCs) at 37 °C but not on ice (see Supplementary Figures S2a,b online). However, incubation of lung leukocytes at 37 °C altered the display of surface molecules, including MHC class II and CD115 (macrophage colony-stimulating factor receptor), on DCs and monocytes, respectively (see Supplementary Figures S2c,d online). This precluded the simultaneous analysis of CCR7 together with certain other molecules. To circumvent this problem and to study *Ccr7* expression under a variety of conditions without altering cellular phenotypes, we generated *Ccr7* reporter mice in which the green fluorescent protein (GFP) coding region replaces that of *Ccr7* (see Supplementary Figures S2f–i online). These mice provided a rapid and temperature-independent method to study *Ccr7* expression (see Supplementary Figure S2e online). On lung DCs, a much higher proportion of CD103⁺ DCs expressed *Ccr7-gfp* than did CD11b^{hi} DCs (Figure 2b), in agreement with the migratory capacities of these two DC subsets.

To determine whether the relatively small proportion of CD11b^{hi} DCs expressing *Ccr7* is an intrinsic property of these cells or simply due to their being shielded from LPS exposure *in vivo*, we purified GFP-negative CD11b^{hi} and CD103⁺ DCs from the lungs of *Ccr7^{gfp}* mice and stimulated the cells *ex vivo* with LPS. This treatment increased the proportion of *Ccr7-gfp*-expressing cells in both DC subsets but did so more effectively in CD103⁺ DCs (Figure 2c). This result indicates that the difference in *Ccr7* expression between the two major lung DC subsets is likely due to intrinsic differences in their potential to express *Ccr7* and not to their anatomical location in the lung.

We next analyzed DCs of mLNs in *Ccr7^{gfp}* mice. We found that a larger proportion of CD103⁺ DCs expressed *Ccr7-gfp* than did CD11b^{hi} DCs (Figure 2d). However, when we restricted our analysis to PKH⁺ DCs that had migrated from the lung, the frequency of CCR7-GFP⁺ DCs was comparable between the CD11b^{hi} and CD103⁺ subsets. This finding is in agreement with the requirement of CCR7 for migration of CD103⁺ and CD11b^{hi} DCs to draining LNs (Figure 1f).

CD14^{hi} and Ly-6C^{hi} CD11b^{hi} DCs do not express *Ccr7* or migrate to mLNs

To better characterize the migratory properties of CD11b^{hi} DCs, we studied subpopulations of DCs in this subset. We first investigated inflammatory DCs, a subset of CD11b^{hi} DCs that are derived from monocytes and are rapidly recruited to the airways by pro-inflammatory stimuli.¹⁵ As remnants of their monocytic heritage, inflammatory mDCs express high levels of Ly-6C.^{15,37,38} To determine whether these cells are migratory, we instilled LPS or polyinosinic-polycytidylic acid (poly (I:C)) into the airways of *Ccr7^{gfp}* mice. As expected, many CD103⁺ DCs and a population of CD11b^{hi} DCs that expressed high levels of MHC class II also expressed *Ccr7-gfp* (Figure 3a). However, Ly-6C^{hi}CD11b^{hi} inflammatory DCs expressed very low levels of *Ccr7-gfp* compared with Ly-6C^{lo}CD11b^{hi} DCs (Figure 3b). These data indicate that the Ly-6C^{hi} inflammatory DCs that are rapidly recruited to the lung by pro-inflammatory stimuli do not express high levels of *Ccr7*.

In addition to inflammatory DCs, monocytes are reported to give rise to CD11b^{hi} DCs that express high levels of the LPS co-receptor, CD14, even during steady-state conditions.^{16,29,30} We found that *Ccr7-gfp* was expressed in CD11b^{hi} DCs displaying intermediate or low levels of CD14 (CD14^{med/lo}) DCs but not in CD14^{hi} DCs (Figure 3c). Thus, neither Ly-6C^{hi} inflammatory DCs nor CD14^{hi}CD11b^{hi} DCs express high levels of *Ccr7*.

The low expression of *Ccr7* seen in CD14^{hi}CD11b^{hi} DCs might have been due to a constraint imposed on them during their differentiation from monocytes. Alternatively, the anatomical location of these cells within the lung might have shielded them from signals that promote *Ccr7* expression. To distinguish between these possibilities, we purified CCR7-GFP-negative DCs from the lungs of untreated *Ccr7^{gfp}* mice and fractionated the cells into three subsets: CD103⁺ DCs, CD14^{med/lo}CD11b^{hi} DCs, and CD14^{hi}CD11b^{hi} DCs. The cells were cultured in the presence of LPS to promote their maturation and induce *Ccr7*. Increased display of CD86 confirmed maturation of almost all DCs in these cultures. Most CD103⁺ DCs, as well as most CD14^{med/lo}CD11b^{hi} DCs, displayed marked increase in CCR7-GFP. By contrast, very little increase in CCR7-GFP was seen for CD14^{hi}CD11b^{hi} DCs (Figures 3d,e). This result suggests that CD14^{hi}CD11b^{hi} DCs in the lung do not express *Ccr7*, even after their activation with LPS.

Absence of Ly-6C^{hi} CD11b^{hi} DCs does not diminish lung DC migration

Ly-6C and CD14 are displayed on moDCs,^{15,16,37,38} but it is unclear whether these markers define distinct populations of moDCs. To address this question, we instilled LPS into the airways of mice to induce pulmonary inflammation and followed the surface marker profile of CD11b^{hi} DCs over time. In the lungs of untreated mice, very few Ly-6C^{hi} inflammatory DCs were seen, and CD11b^{hi} DCs were comprised of CD14^{hi} and CD14^{med/lo} cells (Figures 4a,b). The CD14^{hi} DCs likely represented moDCs, which were previously reported to reside in the lung even during steady-state conditions.^{29,30} Within one day of OVA/LPS instillation, we observed a rapid rise in total DCs, with most of these being Ly-6C^{hi} inflammatory DCs that were readily distinguished from the other two populations of CD11b^{hi} DCs. By day 3 post-OVA/LPS instillation, the number of Ly-6C^{hi} inflammatory DCs in the lung had declined rapidly, and a corresponding increase was seen in CD14^{hi}Ly-6C^{lo} and CD14^{med/lo}Ly-6C^{lo} DCs. This trend continued over the next several days. Thus, inflammatory DCs are relatively short-lived, compared with the other CD11b^{hi} DC subsets.

Rapid and robust accumulation of Ly-6C^{hi} inflammatory DCs to the inflamed lung is mediated largely by the chemokine receptor, CCR2.^{15,37,39} Analysis of *Ccr2*-deficient mice (see Supplementary Figures S3a–e online) revealed that during steady-state conditions, these mice have as many or more CD11b^{hi} and CD103⁺ pulmonary DCs as wild-type mice (Figure 4c). However, after instillation of OVA/LPS, *Ccr2*^{-/-} mice have reduced CD11b^{hi} DCs. This reduction is due largely to a paucity of Ly-6C^{hi} inflammatory DCs, which are recruited in large numbers to the lungs of wild-type mice following OVA/LPS installation (Figure 4d). The other DC subsets, CD103⁺ DCs, CD14^{hi}Ly-6C^{lo} DCs, and CD14^{med/lo}Ly-6C^{lo} DCs, were comparable between *Ccr2*^{-/-} mice and wild-type mice or even slightly increased in the former strain (Figure 4d). We next studied how the absence of inflammatory moDCs in *Ccr2*^{-/-} mice affected overall levels of *Ccr7* expression in DCs. Wild-type and *Ccr2*^{-/-} mice were treated with LPS, and CD11b^{hi} and CD103⁺ DCs were purified by cell sorting. No differences in *Ccr7* expression were seen for CD103⁺ DCs, an expected result because these DCs are present at similar numbers in these two mouse strains. However, CD11b^{hi} DCs from *Ccr2*^{-/-} mice had much higher levels of *Ccr7* than their counterparts in wild-type mice. This result is consistent with the low levels of *Ccr7* expression in inflammatory DCs (Figure 3b) and suggests that large number of

inflammatory DCs in LPS-treated wild-type mice dilutes overall expression of this gene in CD11b^{hi} DCs, whereas this effect is not seen in *Ccr2*^{-/-} mice because they lack inflammatory DCs (Figure 4e). In agreement with this interpretation, we found that the number of migratory, PKH⁺ CD11b^{hi} DCs was higher in mLNs of *Ccr2*^{-/-} mice than in wild-type mice (Figure 4f). Taken together, these observations provide additional evidence that Ly-6C^{hi} inflammatory DCs are non-migratory.

CD14^{hi} and Ly-6C^{hi} CD11b^{hi} DCs in the lung are non-migratory

Our experiments thus far suggested that CD11b^{hi} DCs in the lung are comprised of migratory CD14^{med/lo} DCs and non-migratory Ly-6C^{hi} inflammatory DCs and CD14^{hi} DCs. To confirm this, LPS instillation was used to recruit inflammatory DCs to the lung, and these cells, as well as the other DCs in the lung, were labeled by instillation of PKH (Figure 5a). On the following day, the lungs and mLNs were excised and analyzed for the presence of PKH-labeled DCs. In the lung, the majority of PKH⁺CD11b^{hi} DCs were Ly-6C^{hi} inflammatory DCs (Figure 5b, top). However, in mLNs, almost all PKH⁺ CD11b^{hi} DCs were CD14^{med/lo}Ly-6C^{lo} DCs (Figure 5b, middle). To circumvent possible differences in the ability of various pulmonary DC subsets to be labeled with PKH, we calculated a migration index based on the ratio of PKH⁺CD11b^{hi} DCs in mLNs to PKH⁺CD11b^{hi} DCs in the lung (Figure 5b, bottom). This calculation confirmed that CD14^{med/lo}Ly-6C^{lo} pulmonary DCs are migratory, whereas CD14^{hi} DCs and Ly-6C^{hi} DCs are much less migratory. Thus, inflammatory DCs are rapidly recruited to the lung following LPS inhalation, but they do not migrate to draining LNs. In agreement with this observation, CCR7-GFP was seen in the Ly-6C^{lo} population of CD11b^{hi} DCs in mLNs but not in the Ly-6C^{hi} population in mLNs (Figure 5c).

Previous reports have shown that substantial numbers of Ly-6C^{hi} inflammatory DCs are present in mLNs in the setting of acute inflammation,³⁷ although it has been unclear whether these cells emigrated from the lung. To test the possibility that a stronger pro-inflammatory stimulus is required to promote Ly-6C^{hi} inflammatory DC migration to mLNs, we instilled 0.1 or 10 μ g of LPS into the airways of mice. The recruited inflammatory DCs were subsequently labeled with PKH and their migration to mLNs assessed on the following day. The high-dose LPS led to a robust increase in total Ly-6C^{hi}CD11b^{hi} DCs in mLNs compared with treatment with the low-dose LPS (Figure 5d). However, very few of these DCs were stained with PKH; almost all of the PKH⁺ CD11b^{hi} DCs in the LN were Ly-6C^{lo} (Figure 5e). These results suggest that inflammatory DCs do not migrate from the lung to mLNs, even in the setting of acute inflammation.

The increase in non-migratory, Ly-6C^{hi} DCs in mLNs of LPS-treated mice prompted us to investigate the origin of these cells. Ly-6C^{hi} monocytes were prepared from BM, labeled with CFSE, and transferred into mice that had received instillations of either low- or high-dose LPS. In mice given low-dose LPS, relatively few CFSE-labeled Ly-6C^{hi} monocytes were seen in mLNs. However, in mice given high-dose LPS, these cells were markedly increased (Figure 5f). Together, these data suggest that the Ly-6C^{hi} inflammatory DCs that accumulate in mLNs during acute inflammation are not migratory DCs arriving from the lung but are descendants of monocytes recruited directly from the blood to mLNs.

Our findings with moDCs in the lung were in apparent contrast to a previous report indicating CCR7-dependent accumulation of moDCs in skin-draining LNs.¹⁶ In agreement with that study, we found that after systemic LPS injection into *Ccr7*^{flp} mice, skin-draining LNs contained many *Ccr7*^{flp}-expressing CD11b^{hi} DCs, CD14^{hi} DCs, and CD103⁺ DCs but no *Ccr7*^{flp}-expressing Ly-6C^{hi} inflammatory DCs (see Supplementary Figures S4a,b online). We also confirmed that some *in vitro* generated moDCs also have the capacity to express *Ccr7* (see Supplementary Figures S4c–e online). Together, these data suggest that

inflammatory DCs do not express *Ccr7*, but its expression in CD14^{hi} DCs is tissue-dependent.

Ly-6C^{hi} and CD14^{hi} DCs are monocyte-derived and develop independently of FLT3L

We next investigated whether the diverse migratory potential of the various CD11b^{hi} DC subpopulations in the lung was related to their developmental pathways. We reasoned that *Flt3L*^{-/-} mice would be useful in this regard because these mice lack CDPs,^{25,26,40} which can differentiate into cDCs^{25,26} but not monocytes. *Flt3L*^{-/-} mice also lack CD103⁺ DCs,²⁷ a finding that we confirmed for untreated and OVA/LPS-treated mice (Figure 6a). However, we noticed that the lungs of *Flt3L*^{-/-} mice do contain CD11b^{hi} DCs, albeit at a slightly reduced number compared with wild-type mice. More detailed analysis revealed that during steady-state conditions, pulmonary CD11b^{hi} DCs in *Flt3L*^{-/-} mice are comprised almost exclusively of the CD14^{hi} subset, with very few CD14^{med/lo} DCs (Figure 6b). Upon stimulation with OVA/LPS, Ly-6C^{hi} DCs accumulated in the lungs of *Flt3L*^{-/-} mice to a similar extent as in wild-type mice, whereas the number of CD14^{med/lo} DCs remained low. These data suggest that the CD14^{med/lo}CD11b^{hi} DCs lacking in *Flt3L*^{-/-} mice are likely CDP-derived, whereas Ly-6C^{hi} DCs and CD14^{hi}CD11b^{hi} DCs are monocyte-derived.

To confirm that monocytes give rise to Ly-6C^{hi} inflammatory DCs and CD14^{hi} DCs, we prepared Ly-6C^{hi} inflammatory monocytes (CD11b⁺Ly-6C^{hi}CD115⁺CD11c⁻I-A⁻) (see Supplementary Figures S5a, b and Supplementary Methods online) from the BM of CD45.1 mice and adoptively transferred these cells to CD45.2-recipient mice, whose airways had been instilled with OVA/LPS before the monocyte transfer. By gating on CD45.1⁺I-A⁺CD11c⁺ cells, we were able to follow the fate of moDCs in the lung (Figure 6c). At one day post-transfer, almost all of these cells were Ly-6C^{hi} inflammatory DCs. Over time, the total number of donor moDCs in the lung declined, and CD14^{hi} DCs became dominant population (Figures 6c,d). Importantly, very few Ly-6C^{lo}CD14^{med/lo} DCs were seen within the CD45.1⁺ gate, suggesting that monocytes give rise to Ly-6C^{hi} inflammatory DCs and CD14^{hi}CD11b⁺ DCs but not to Ly-6C^{lo}CD14^{med/lo}CD11b⁺ DCs.

Migratory DCs in the lung are FLT3/FLT3L-dependent cDCs

Our experiments with PKH staining of pulmonary DCs had shown that CD14^{hi} moDCs were significantly less migratory than CD14^{med/lo} cDCs. Nonetheless, we did detect some PKH⁺ CD14^{hi} DCs in mLN (Figure 5b). Although display levels of CD14 are useful to distinguish CD14^{hi} moDCs from CD14^{med/lo} cDCs, these populations were not widely separated in our cytograms, leaving open the possibility that there is some overlap in CD14 expression between CDP-derived and monocyte-derived CD11b^{hi} DCs. To independently study the migration of these two DC subsets, we carried out a series of experiments with *Flt3L*-deficient mice, which had a dramatic reduction in CD14^{med/lo}CD11b^{hi} DCs but normal levels of CD14^{hi}CD11b^{hi} DCs (Figure 6b). The latter appeared to be mature, as judged by their high levels of CD86 and I-A (see Supplementary Figure S5c online) and by the presence of dendrites (see Supplementary Figure S5d online). Furthermore, total lung DCs from *Flt3L*^{-/-} mice efficiently stimulated naive CD4⁺ T-cell differentiation to Th1 cells, as measured by production of IFN- γ (see Supplementary Figure S5e online). The latter finding is in agreement with previous reports showing preferential Th1 induction by moDCs.^{16,37,38} Th2 induction by total DCs prepared from *Flt3L*^{-/-} mice was impaired, likely because they lack CD103⁺ DCs, which efficiently prime Th2 differentiation.¹³ Thus, based on their expression of MHC class II, DC-like morphology, and T-cell-stimulating capability, we concluded that CD14^{hi}CD11b^{hi} cells in the *Flt3L*^{-/-} mouse lungs are likely functional moDCs, and that *Flt3L*^{-/-} mice are a useful genetic model for studying migratory and functional properties of moDCs *in vivo*.

Having confirmed that the CD11b^{hi} DCs in *Flt3L*^{-/-} mice are restricted to moDCs, we investigated *Ccr7* expression in lung DCs in these animals. CD11b^{hi} DCs from *Flt3L*^{-/-} mice did not express appreciable levels of *Ccr7* mRNA (Figure 7a). Moreover, whereas PKH-labeled CD11b^{hi} DCs from wild-type mice readily migrated to mLNs, CD11b^{hi} DCs counterparts from *Flt3L*^{-/-} mice did not, even when low-(0.1 μg) or high-dose (10 μg) LPS (Figures 7b,c) was instilled to induce inflammation. The virtual absence of PKH⁺ migratory CD11b^{hi} DCs in mLNs of *Flt3L*^{-/-} mice was probably not related to unanticipated changes in the lymphatics or the LNs of these animals, because *in vitro*-generated wild-type BMDCs migrated from the airway to mLNs of *Flt3L*^{-/-} and wild-type-recipient mice with comparable efficiencies (Figure 7d). To confirm that FLT3/FLT3L interactions are required for the development of migratory DCs, we tested lung DC migration in chimeric mice in which wild-type mice received a mixture of BM from genetically marked wild-type (CD45.2) and *Flt3*^{-/-} donor (CD45.1) mice. PKH was instilled into the airways of these chimeric mice so that we could follow migration of both types of donor-derived DCs to mLNs. As expected, PKH⁺ CD103⁺ DCs in the lung and LNs of these chimeric mice were derived exclusively from wild-type (CD45.2) mice because FLT3 is required for the development of these cells (Figures 7e-g). By contrast, PKH⁺ CD11b^{hi} DCs in the lungs of the chimeric mice were derived almost equally from wild-type and *Flt3*^{-/-} donors. Despite that, almost all PKH⁺ CD11b^{hi} DCs in mLNs of the chimeric mice were derived from wild-type donors. Thus, although *Flt3*^{-/-} CD11b^{hi} moDCs develop normally and accumulate in the lung, they do not readily migrate to mLNs. Based on these results, we conclude that in the lung, migratory DCs are comprised almost exclusively of FLT3- and FLT3L-dependent cDCs, and that FLT3- and FLT3L-independent moDCs are intrinsically non-migratory.

DISCUSSION

Lung-resident DCs are well-known to take up inhaled antigens and migrate to draining LNs for presentation of antigen-derived peptides to naive T cells. However, in experimental models of asthma DCs are also required during the challenge phase,^{8,9} suggesting that some DCs have evolved to remain in the lung and activate antigen-specific memory cells recruited to the lung upon secondary exposure to antigens. For example, lung-resident DCs are required to trigger release of inflammatory mediators by influenza-specific CD8⁺ T cells during the late phase of influenza infection, after most of the virus has been cleared.⁴¹ Thus, non-migratory, lung-resident DCs might provide important functions during recall responses to antigen challenge. If so, reducing or preventing the accumulation of these cells in the inflamed lung might diminish the pathological inflammation seen in these and other diseases.

It has been unclear whether the migration of individual DCs is stochastic, determined solely by exposure to pro-inflammatory stimuli or cytokines, or whether some DCs are programmed to remain in the lung. Resolving this issue should provide important clues to the primary functions of DC subsets. Our present findings reveal that in the lung, most cDCs, including CD103⁺ DCs and the CD14^{med/lo} subset of CD11b^{hi} DCs, are capable of expressing *Ccr7* and migrating from the lung to mLNs, whereas moDCs do not express this receptor and do not migrate to draining LNs.

We found that compared with lung-resident CD103⁺ DCs, fewer CD11b^{hi} DCs expressed *Ccr7* after stimulation with LPS *in vivo*. This difference was largely due to the virtual absence of *Ccr7* expression on the monocyte-derived subset of CD11b^{hi} DCs. In fact, CD14^{hi} moDCs failed to express *Ccr7*, even after their purification from the lung and culture with LPS-containing media, whereas *Ccr7* was strongly increased under these conditions in CD14^{med/lo}CD11b^{hi} cDCs and in CD103⁺ cDCs. This finding argues against the hypothesis that the inability of CD14^{hi} moDCs to increase *Ccr7* expression is due solely to their

anatomical positioning within the lung. Rather, our data suggest that the migratory properties of lung DCs are intrinsically programmed. Not all CD11b^{hi} cDCs and CD103⁺ cDCs were CCR7-GFP⁺ after their overnight culture with LPS-containing media, but it is likely that *Ccr7* expression had declined in some cells by the end of the culture period. This idea is supported by our finding that only half of PKH⁺ migratory DCs in draining LNs were CCR7-GFP⁺, even though the migration of these cells is critically dependent on CCR7 and occurred during the 24 h between the labeling of these cells in the lung and their analysis in the LN. Thus, *Ccr7* might be expressed only long enough to allow DC migration from the lung to T-cell zones in draining LNs.

Our present data suggest that the absence of *Ccr7* expression in moDCs was not due solely to a lack of maturity because this receptor was absent not only in inflammatory DCs, but also in CD14^{hi}CD11b^{hi} DCs in wild-type mice during steady-state conditions and in all CD11b^{hi} moDCs from *Flt3L*^{-/-} mice. Apart from their levels of *Ccr7* expression, the latter DCs appeared fully mature, as determined by their high display levels of MHC class II and co-stimulatory molecules, their DC-like morphologies, and their ability to stimulate naive T-cell differentiation. Therefore, the absence of *Ccr7* expression in moDCs is likely an intrinsic property of these cells and related to their descent from monocytes. The migratory differences between CD11b^{hi} moDCs and CD11b^{hi} cDCs might help to reconcile previous reports that came to different conclusions regarding the migratory properties of pulmonary CD11b^{hi} DCs.^{3,20,21,42,43} Although the signaling pathways that control *Ccr7* expression are not yet well understood, a comparison of the transcriptional and epigenomic status of CD11b^{hi} cDCs and moDCs will likely be informative in this regard.

Our finding that moDCs in the lung lack *Ccr7* expression and are non-migratory is in apparent contrast with previous reports showing that moDCs can accumulate in LNs in a CCR7-dependent manner upon systemic administration of LPS¹⁶ and that *Ccr7* is expressed on Langerhans cells,⁴⁴ which are monocyte-derived.⁴⁵ We also confirmed that BM monocytes can differentiate into *Ccr7*-expressing DCs. Thus, not all moDCs lack *Ccr7*. It is possible that the microenvironment of the lung—and perhaps other tissues—provide signals that suppress *Ccr7* expression in moDCs. Although in most cases the identities of such putative signals are unknown, there are several precedents for phenotypic differences among DCs of different tissues. For example, Langerhans cells are present only in the skin, and CD103⁺CD11b⁺ double-positive cells are found in large numbers in the lamina propria of the gut but are rare in the lung.^{13,28} Interestingly, these double-positive cells, which are CX3CR1⁻, express *Ccr7* and migrate to gut-draining LNs, whereas CD103⁻ CX3CR1⁺ DCs in the lamina propria are non-migratory.^{28,46} To date, there have been no reports of CD103⁻CD11b^{hi} migratory cDCs in the gut that are similar to those that we have found in the lung. It is possible that the CD11b⁺CD103⁺ double-positive DCs in the gut are functionally analogous to CD14^{med/lo}CD11b^{hi} cDCs in the lung, and that the phenotypic differences between these DC populations result from distinct signals provided by the different micro-environments in those organs. These observations imply that phenotypes of DCs are largely, but not entirely, determined during lineage differentiation. Identification of molecular signals in non-lymphoid tissue that act to fine tune functions of DCs will likely be an important area of future research in DC biology.

METHODS

Mice

C57BL/6, *Ccr7*^{-/-}, CD45.1 and OT-II TCR transgenic mice were purchased from Jackson Laboratories (Bar Harbor, ME). *Flt3L*^{-/-} mice and control C57BL/6 mice were from Taconic (Germantown, NY). *Ccr7*^{gfp} and *Ccr2*^{-/-} targeted insertion reporter mice on a C57BL/6 background were generated at Xenogen (Caliper Life Sciences, Hopkinton, MA)

through a contractual arrangement with the NIEHS (see Supplementary Figures S2 and S3 online). *Flt3*^{-/-} mice originally generated by Ihor Lemischka (Mount Sinai School of Medicine) were provided by Michel Nussenzweig (Rockefeller University). Mice were housed in specific pathogen-free conditions at the NIEHS or Rockefeller University and used between 6 and 12 weeks of age in accordance with guidelines provided by the Institutional Animal Care and Use Committees.

Mouse sensitization and cell-tracker administration

Mice were anesthetized by isoflurane inhalation and given 100 µg endotoxin-free OVA (Profos AG, Germany), alone or together with 0.1 µg LPS (Sigma, St Louis, MO) or with 1 µg poly (I:C) (InvivoGen, San Diego, CA) unless otherwise specified. Instillations of reagents were done by oropharyngeal aspiration as described previously.⁴⁷ In some experiments, DCs were labeled *in vivo* by instillations of 50 µl of 10 µm PKH26 (Sigma) or CFSE (Invitrogen, Grand Island, NY) 24 h before OVA/LPS instillation unless specified. OVA-bearing DCs were identified by instillation of endotoxin-free OVA labeled with Alexa Fluor 647 (Invitrogen). For skin-draining DC analysis, 200 µl phosphate-buffered saline containing 0.1 µg LPS was injected into mouse tail veins 24 h before tissue harvest. To examine cell-tracker dye-induced airway inflammation, bronchoalveolar lavage was performed on mice 24 h after instillation of cell trackers, and the cells were counted under a microscope.

Preparation and analysis of pulmonary DCs

DCs from the mouse lungs and mLNs were prepared as described previously.¹³ Cells were diluted to $2 \times 10^6/100 \mu\text{l}$ and incubated with a non-specific-binding blocking reagent cocktail of anti-mouse CD16/CD32 (2.4G2), normal mouse, and rat serum (Jackson ImmunoResearch, West Grove, PA) for 5 min. For staining of surface antigens, cells were incubated with fluorochrome (Allophycocyanin (APC), APC-Cy7, Alexa Fluor 488, Alexa Fluor 647, eFluor 450, eFluor 605 NC, FITC, PerCP-Cy5.5 or Phycoerythrin), or biotin-conjugated antibodies against mouse CD3e (145-2C11), CD11b (M1/70), CD11c (N418 and HL3), CD14 (Sa2-8), CD19 (6D5), CD45.1 (A20), CD86 (GL1), CD103 (M290), CD115 (AFS98), CD117/c-Kit (2B8), CD197/CCR7 (4B12), Ly-6C (AL-21), Ly-6G (1A8), MHC class II I-A^b (AFb.120), MMR (MR5D3) and Siglec-F (BD Biosciences (San Jose, CA), BioLegend (San Diego, CA) and eBioscience (San Diego, CA)). Staining with biotinylated antibodies was followed by fluorochrome-conjugated streptavidin. Stained cells were analyzed on a 5 laser LSRII, or sorted on a 5 laser ARIA-II flow cytometer (BD Biosciences), and the data analyzed using FACS Diva (BD Bioscience) and FlowJo software (Treestar, Ashland, OR). Dead cells were excluded based on their forward and side scatter. Only single cells were analyzed. In some experiments, DC subsets were purified and cultured in complete RPMI1640 (cRPMI) containing 100 ng ml^{-1} LPS (Sigma), in addition to 10% fetal bovine serum (Gemini, West Sacramento, CA), penicillin/streptomycin (Invitro-Gen) and 50 ng ml^{-1} β -mercaptoethanol (Sigma). In some experiments, cells from purified subsets were centrifuged onto glass slides and photographed using an Olympus BX51 microscope, DP70 digital camera, and DP software (Olympus, Center Valley, PA).

Purification of monocytes and *in vitro* generation of DCs

Inflammatory monocytes (CD3⁻CD11b⁺CD19⁻CD49b⁻I-A⁻Ly-6C^{hi}Ly-6G⁻TER119⁻7-AAD⁻) from BM were enriched using an automated magnet-activated cell sorter (Miltenyi, Auburn, CA) and then further purified by flow cytometry-based sorting. To prepare BMDCs, marrow was collected, RBCs lysed with 0.15 M ammonium chloride and 1 mM potassium bicarbonate, and the cells cultured in cRPMI containing 5 ng ml^{-1} GM-CSF (granulocyte macrophage colony-stimulating factor; R&D Systems) for 9 days. To generate moDCs *in vitro*, purified BM monocytes were cultured in cRPMI containing 5 ng ml^{-1} GM-

CSF and IL-4 (R&D Systems). After 4 or 7 days of culture, cells were harvested and analyzed by flow cytometry or microscopy as described above.

BM chimera mice

BM chimeric mice were generated using a mixture of BM cells from C57BL/6 (CD45.2) and *Flt3*^{-/-} (CD45.1) mice at 4:6 ratio that was intravenously injected into tail veins of 9 Gy γ -ray-irradiated C57BL/6 mice (10^7 cells/recipient) 6 weeks before experiment.¹⁶

Adoptive transfer of cells

For BMDC migration assays, 10^6 CD11c⁺I-A⁺ DCs from CD45.1⁺ mice were instilled into airways of recipient CD45.2⁺ mice, and the efficiency of migration to mLNs assessed by quantitation of CD45.1⁺ donor DCs in mLNs. For monocyte fate studies, 6×10^5 purified monocytes were intravenously injected into mouse tail veins.

Co-culture of naive T cells with DCs

Naive CD4⁺ T cells were prepared from pools of LNs and spleens of OT-II TCR transgenic mice as previously described.¹³ DCs were purified by flow cytometric sorting¹³ from the lungs of mice that had received OVA/LPS 16 h earlier. The OT-II T cells (10^5 /well) were cultured together with lung DCs (5×10^4 /well) in a 5% CO₂ incubator in 200 μ l Iscove's modified Dulbecco's medium containing 10% fetal bovine serum (certified, Invitrogen), 50 μ M β -mercaptoethanol, penicillin, and streptomycin in a 96-well U-bottom plate (BD Biosciences). After 5 days of the primary co-culture, T cells (10^5 /well) were transferred to a 96-well flat-bottomed plate coated with 1 μ g ml⁻¹ anti-CD3 ϵ and 5 μ g ml⁻¹ anti-CD28 antibodies (eBioscience), and IFN- γ or IL-13 in the cell supernatants were analyzed 24 h later by enzyme-linked immunosorbent assay as measures of Th1 and Th2 induction, respectively.

Quantitative PCR

Total RNA was isolated from sorted DCs using RNeasy kit (Qiagen, Valencia, CA) and converted to cDNA with oligo dT primers and SuperScript III First Strand kit (Invitrogen). PCR amplification was performed using TaqMan primers and probes (Applied Biosystems, Foster City, CA) for mouse *Ccr7* (assay ID: Mm01301785_m1) and *Gapdh* (assay ID: Mm99999915_g1) with TaqMan PCR Master Mix (Applied Biosystems) and Mx3000P QPCR system (Agilent Technologies, Santa Clara, CA). The relative expression level of each gene was determined according to the manufacturer's instruction and normalized to *Gapdh* expression.

Statistics

Data are expressed as mean \pm s.e.m. Statistical differences between groups were calculated using a two-tailed Student's *t*-test, unless indicated otherwise. *P*<0.05 was considered significant.

Supplementary Material

Refer to Web version on PubMed Central for supplementary material.

Acknowledgments

We thank Maria Sifre for help with flow cytometry, Ligon Perrow for support with animal experiments, and Michael Fessler and Kym Gowdy (NIEHS) for critical reading of the manuscript. This work was supported by the Intramural Research Program of the National Institutes of Health and the National Institute of Environmental Health Sciences.

References

1. Steinman RM. Lasker Basic Medical Research Award. Dendritic cells: versatile controllers of the immune system. *Nat Med.* 2007; 13:1155–1159. [PubMed: 17917664]
2. Lambrecht BN, Hammad H. Lung dendritic cells in respiratory viral infection and asthma: from protection to immunopathology. *Annu Rev Immunol.* 2012; 30:243–270. [PubMed: 22224777]
3. Jakubzick C, et al. Lymph-migrating, tissue-derived dendritic cells are minor constituents within steady-state lymph nodes. *J Exp Med.* 2008; 205:2839–2850. [PubMed: 18981237]
4. Vermaelen KY, Carro-Muino I, Lambrecht BN, Pauwels RA. Specific migratory dendritic cells rapidly transport antigen from the airways to the thoracic lymph nodes. *J Exp Med.* 2001; 193:51–60. [PubMed: 11136820]
5. Desch AN, et al. CD103 + pulmonary dendritic cells preferentially acquire and present apoptotic cell-associated antigen. *J Exp Med.* 2011; 208:1789–1797. [PubMed: 21859845]
6. Julia V, et al. A restricted subset of dendritic cells captures airborne antigens and remains able to activate specific T cells long after antigen exposure. *Immunity.* 2002; 16:271–283. [PubMed: 11869687]
7. GeurtsvanKessel CH, et al. Dendritic cells are crucial for maintenance of tertiary lymphoid structures in the lung of influenza virus-infected mice. *J Exp Med.* 2009; 206:2339–2349. [PubMed: 19808255]
8. Lambrecht BN, Salomon B, Klatzmann D, Pauwels RA. Dendritic cells are required for the development of chronic eosinophilic airway inflammation in response to inhaled antigen in sensitized mice. *J Immunol.* 1998; 160:4090–4097. [PubMed: 9558120]
9. van Rijt LS, et al. *In vivo* depletion of lung CD11c + dendritic cells during allergen challenge abrogates the characteristic features of asthma. *J Exp Med.* 2005; 201:981–991. [PubMed: 15781587]
10. Sung SS, et al. A major lung CD103 (alphaE)-beta7 integrin-positive epithelial dendritic cell population expressing Langerin and tight junction proteins. *J Immunol.* 2006; 176:2161–2172. [PubMed: 16455972]
11. del Rio ML, Rodriguez-Barbosa JI, Kremmer E, Forster R. CD103-and CD103 + bronchial lymph node dendritic cells are specialized in presenting and cross-presenting innocuous antigen to CD4 + and CD8 + T cells. *J Immunol.* 2007; 178:6861–6866. [PubMed: 17513734]
12. GeurtsvanKessel CH, et al. Clearance of influenza virus from the lung depends on migratory langerin +CD11b- but not plasmacytoid dendritic cells. *J Exp Med.* 2008; 205:1621–1634. [PubMed: 18591406]
13. Nakano H, et al. Pulmonary CD103(+) dendritic cells prime Th2 responses to inhaled allergens. *Mucosal Immunol.* 2012; 5:53–65. [PubMed: 22012243]
14. Beaty SR, Rose CE Jr, Sung SS. Diverse and potent chemokine production by lung CD11bhigh dendritic cells in homeostasis and in allergic lung inflammation. *J Immunol.* 2007; 178:1882–1895. [PubMed: 17237439]
15. Lin KL, Suzuki Y, Nakano H, Ramsburg E, Gunn MD. CCR2 + monocyte-derived dendritic cells and exudate macrophages produce influenza-induced pulmonary immune pathology and mortality. *J Immunol.* 2008; 180:2562–2572. [PubMed: 18250467]
16. Cheong C, et al. Microbial stimulation fully differentiates monocytes to DC-SIGN/CD209(+) dendritic cells for immune T cell areas. *Cell.* 2010; 143:416–429. [PubMed: 21029863]
17. Forster R, et al. CCR7 coordinates the primary immune response by establishing functional microenvironments in secondary lymphoid organs. *Cell.* 1999; 99:23–33. [PubMed: 10520991]
18. Gunn MD, et al. Mice lacking expression of secondary lymphoid organ chemokine have defects in lymphocyte homing and dendritic cell localization. *J Exp Med.* 1999; 189:451–460. [PubMed: 9927507]
19. Gunn MD, Tangemann K, Tam C, Cyster JG, Rosen SD, Williams LT, et al. A chemokine expressed in lymphoid high endothelial venules promotes the adhesion and chemotaxis of naive T lymphocytes. *Proc Natl Acad Sci USA.* 1998; 95:258–263. [PubMed: 9419363]

20. Hintzen G, et al. Induction of tolerance to innocuous inhaled antigen relies on a CCR7-dependent dendritic cell-mediated antigen transport to the bronchial lymph node. *J Immunol.* 2006; 177:7346–7354. [PubMed: 17082654]
21. Jakubzick C, Tacke F, Llodra J, van Rooijen N, Randolph GJ. Modulation of dendritic cell trafficking to and from the airways. *J Immunol.* 2006; 176:3578–3584. [PubMed: 16517726]
22. Raymond M, et al. Selective control of SIRP-alpha-positive airway dendritic cell trafficking through CD47 is critical for the development of T(H)2-mediated allergic inflammation. *J Allergy Clin Immunol.* 2009; 124:1333–1342. e1331. [PubMed: 19748659]
23. Fogg DK, et al. A clonogenic bone marrow progenitor specific for macrophages and dendritic cells. *Science.* 2006; 311:83–87. [PubMed: 16322423]
24. Varol C, et al. Monocytes give rise to mucosal, but not splenic, conventional dendritic cells. *J Exp Med.* 2007; 204:171–180. [PubMed: 17190836]
25. Naik SH, et al. Development of plasmacytoid and conventional dendritic cell subtypes from single precursor cells derived *in vitro* and *in vivo*. *Nat Immunol.* 2007; 8:1217–1226. [PubMed: 17922015]
26. Onai N, et al. Identification of clonogenic common Flt3 +M-CSFR + plasmacytoid and conventional dendritic cell progenitors in mouse bone marrow. *Nat Immunol.* 2007; 8:1207–1216. [PubMed: 17922016]
27. Ginhoux F, et al. The origin and development of nonlymphoid tissue CD103 + DCs. *J Exp Med.* 2009; 206:3115–3130. [PubMed: 20008528]
28. Bogunovic M, et al. Origin of the lamina propria dendritic cell network. *Immunity.* 2009; 31:513–525. [PubMed: 19733489]
29. Geissmann F, Jung S, Littman DR. Blood monocytes consist of two principal subsets with distinct migratory properties. *Immunity.* 2003; 19:71–82. [PubMed: 12871640]
30. Landsman L, Varol C, Jung S. Distinct differentiation potential of blood monocyte subsets in the lung. *J Immunol.* 2007; 178:2000–2007. [PubMed: 17277103]
31. Jakubzick C, Randolph GJ. Methods to study pulmonary dendritic cell migration. *Methods Mol Biol.* 2010; 595:371–382. [PubMed: 19941125]
32. Stevens WW, Kim TS, Pujanauski LM, Hao X, Braciale TJ. Detection and quantitation of eosinophils in the murine respiratory tract by flow cytometry. *J Immunol Methods.* 2007; 327:63–74. [PubMed: 17716680]
33. Vermaelen K, Pauwels R. Accurate and simple discrimination of mouse pulmonary dendritic cell and macrophage populations by flow cytometry: methodology and new insights. *Cytometry.* 2004; 61:170–177. [PubMed: 15382026]
34. Eisenbarth SC, et al. Lipopolysaccharide-enhanced, toll-like receptor 4-dependent T helper cell type 2 responses to inhaled antigen. *J Exp Med.* 2002; 196:1645–1651. [PubMed: 12486107]
35. Jakubzick C, Helft J, Kaplan TJ, Randolph GJ. Optimization of methods to study pulmonary dendritic cell migration reveals distinct capacities of DC subsets to acquire soluble versus particulate antigen. *J Immunol Methods.* 2008; 337:121–131. [PubMed: 18662693]
36. Horan PK, Melnicoff MJ, Jensen BD, Slezak SE. Fluorescent cell labeling for *in vivo* and *in vitro* cell tracking. *Methods Cell Biol.* 1990; 33:469–490. [PubMed: 2084480]
37. Nakano H, et al. Blood-derived inflammatory dendritic cells in lymph nodes stimulate acute T helper type 1 immune responses. *Nat Immunol.* 2009; 10:394–402. [PubMed: 19252492]
38. Leon B, Lopez-Bravo M, Ardavin C. Monocyte-derived dendritic cells formed at the infection site control the induction of protective T helper 1 responses against *Leishmania*. *Immunity.* 2007; 26:519–531. [PubMed: 17412618]
39. Serbina NV, Pamer EG. Monocyte emigration from bone marrow during bacterial infection requires signals mediated by chemokine receptor CCR2. *Nat Immunol.* 2006; 7:311–317. [PubMed: 16462739]
40. Waskow C, et al. The receptor tyrosine kinase Flt3 is required for dendritic cell development in peripheral lymphoid tissues. *Nat Immunol.* 2008; 9:676–683. [PubMed: 18469816]
41. Hufford MM, Kim TS, Sun J, Braciale TJ. Antiviral CD8 + T cell effector activities *in situ* are regulated by target cell type. *J Exp Med.* 2011; 208:167–180. [PubMed: 21187318]

42. Belz GT, et al. Distinct migrating and nonmigrating dendritic cell populations are involved in MHC class I-restricted antigen presentation after lung infection with virus. *Proc Natl Acad Sci USA*. 2004; 101:8670–8675. [PubMed: 15163797]
43. Lukens MV, Kruijsen D, Coenjaerts FE, Kimpen JL, van Bleek GM. Respiratory syncytial virus-induced activation and migration of respiratory dendritic cells and subsequent antigen presentation in the lung-draining lymph node. *J Virol*. 2009; 83:7235–7243. [PubMed: 19420085]
44. Ohl L, et al. CCR7 governs skin dendritic cell migration under inflammatory and steady-state conditions. *Immunity*. 2004; 21:279–288. [PubMed: 15308107]
45. Merad M, et al. Langerhans cells renew in the skin throughout life under steady-state conditions. *Nat Immunol*. 2002; 3:1135–1141. [PubMed: 12415265]
46. Schulz O, et al. Intestinal CD103 +, but not CX3CR1 +, antigen sampling cells migrate in lymph and serve classical dendritic cell functions. *J Exp Med*. 2009; 206:3101–3114. [PubMed: 20008524]
47. Wilson RH, et al. Allergic sensitization through the airway primes Th17-dependent neutrophilia and airway hyper responsiveness. *Am J Respir Crit Care Med*. 2009; 180:720–730. [PubMed: 19661246]

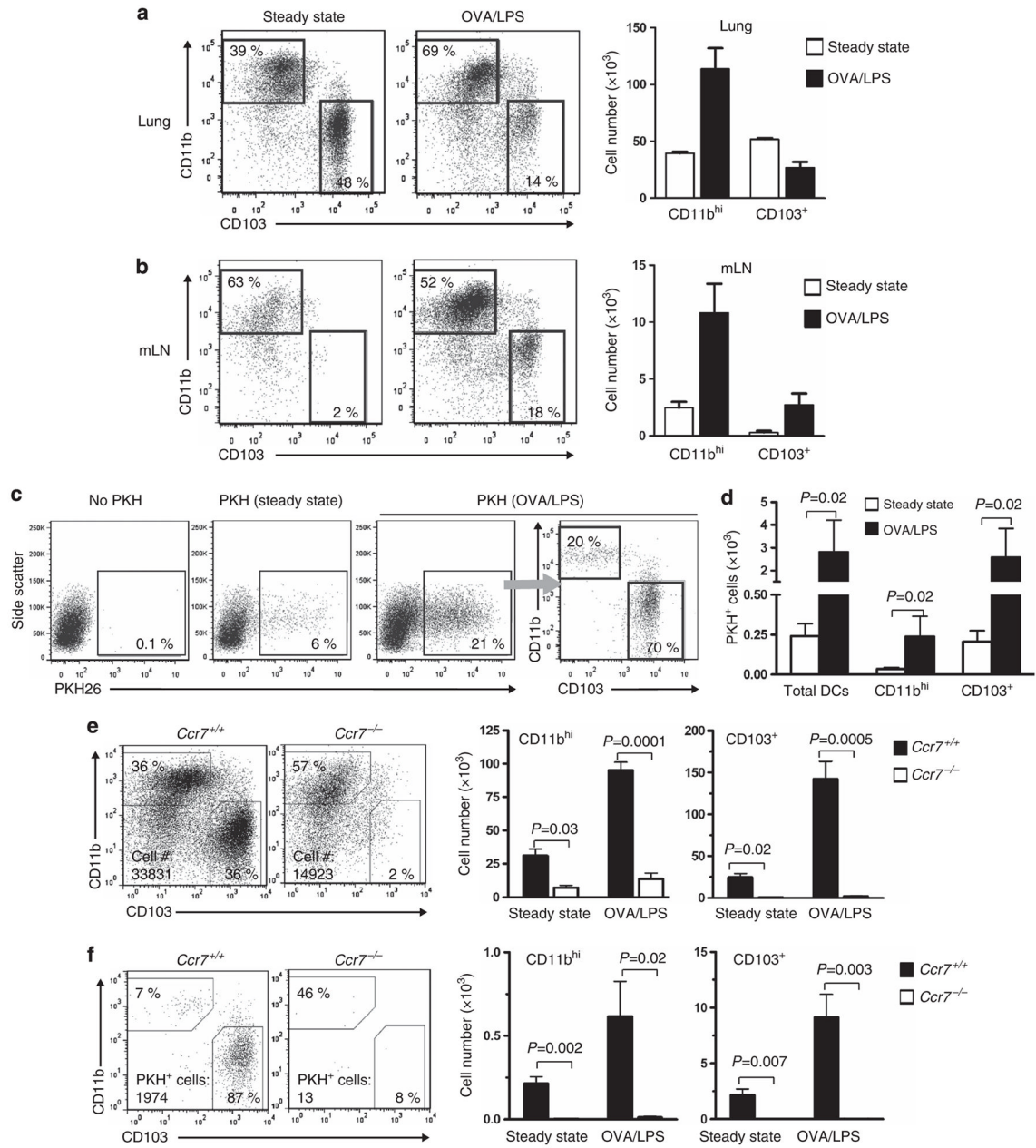


Figure 1. CD103⁺ dendritic cells (DCs) and a subpopulation of CD11b^{hi} DCs migrate to lung-draining mediastinal lymph nodes (mLNs) during allergic sensitization through the airway. **(a, b)** Analysis of CD103⁺ and CD11b^{hi} DCs in the lung **(a)** and mLNs **(b)** under steady-state conditions and 24 h after instillation of ovalbumin/lipopolysaccharide (OVA/LPS). Shown are representative cytograms of DCs from individual mice, as well as bar histograms showing mean values \pm s.e.m. **(c)** Cytograms showing migratory (PKH⁺) DCs in mLNs under steady-state conditions or after instillation of OVA/LPS. **(d)** Compiled data of migratory CD11b^{hi} and CD103⁺ DCs in mLNs. *P*-value by Mann–Whitney test, *n*=4 mice/group. **(e)** Total DCs. Cytogram showing major DC populations in mLNs of wild-type and *Ccr7*^{-/-} mice 24 h after OVA/LPS instillation (left), and histograms showing total number of

CD103⁺ and CD11b^{hi} DCs under steady-state conditions and after OVA/LPS (right). **(f)** Migratory DCs. Representative cytogram showing CD103⁺ and CD11b^{hi} DCs after gating on PKH⁺ migratory DCs and histograms showing numbers of migratory CD103⁺ and CD11b^{hi} DCs in mLNs of Ccr7^{+/+} and Ccr7^{-/-} mice. (*n*=4 mice/group). A representative result of two independent experiments is shown.

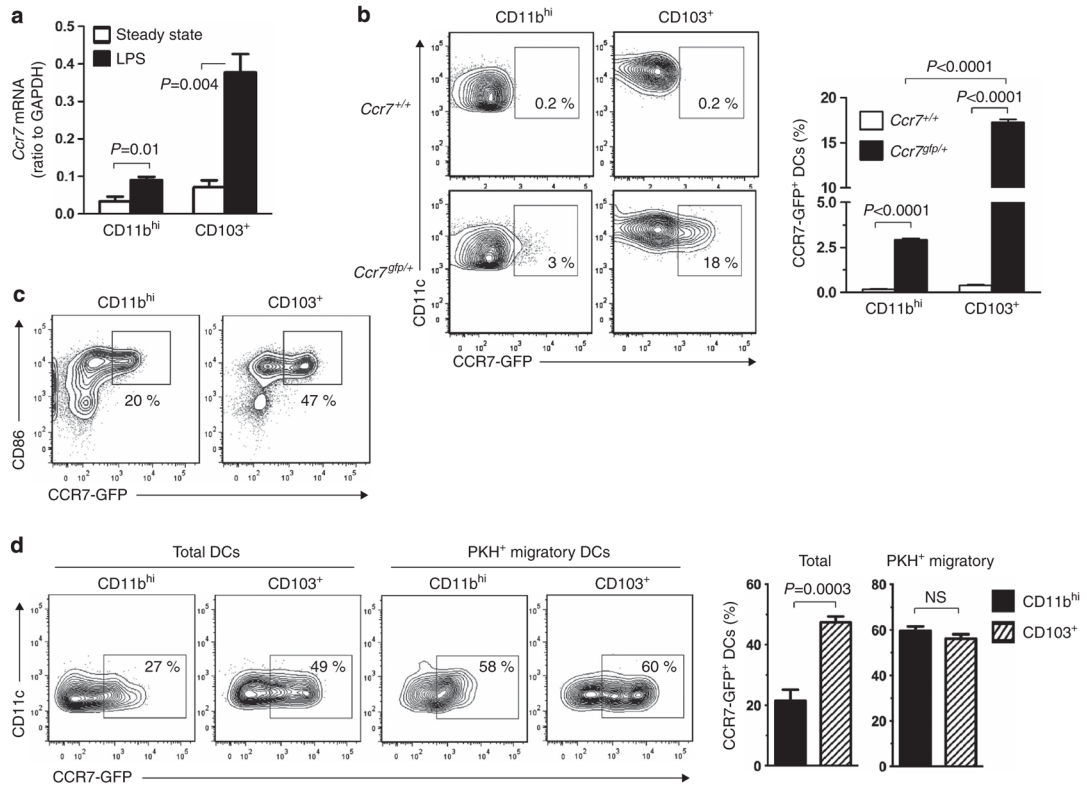


Figure 2. Expression of *Ccr7* in pulmonary dendritic cell (DC) subsets. **(a)** *Ccr7* mRNA in CD103⁺ and CD11b^{hi} lung DCs during steady-state conditions and after lipopolysaccharide (LPS) instillation. **(b)** CCR7-GFP (CCR7-green fluorescent protein) fluorescence in CD103⁺ and CD11b^{hi} DCs from the lungs of *Ccr7*^{gfp/+} mice 24 h after LPS instillation. Shown are representative cytograms of individual mice, as well as bar histograms showing compiled data of four mice per group. **(c)** CCR7-GFP fluorescence in purified CD11b^{hi} and CD103⁺ DCs after 16 h of *ex vivo* culture in LPS (0.1 $\mu\text{g ml}^{-1}$)-containing media. **(d)** CCR7-GFP fluorescence in total and PKH⁺ migratory DCs of the indicated DC subsets prepared from lymph nodes of *Ccr7*^{gfp/+} mice. Representative cytograms of individual mice and bar histograms of compiled data for three mice per group are shown. Data shown are from one of two experiments yielding similar results. GAPDH, glyceraldehyde 3-phosphate dehydrogenase; NS, not significant.

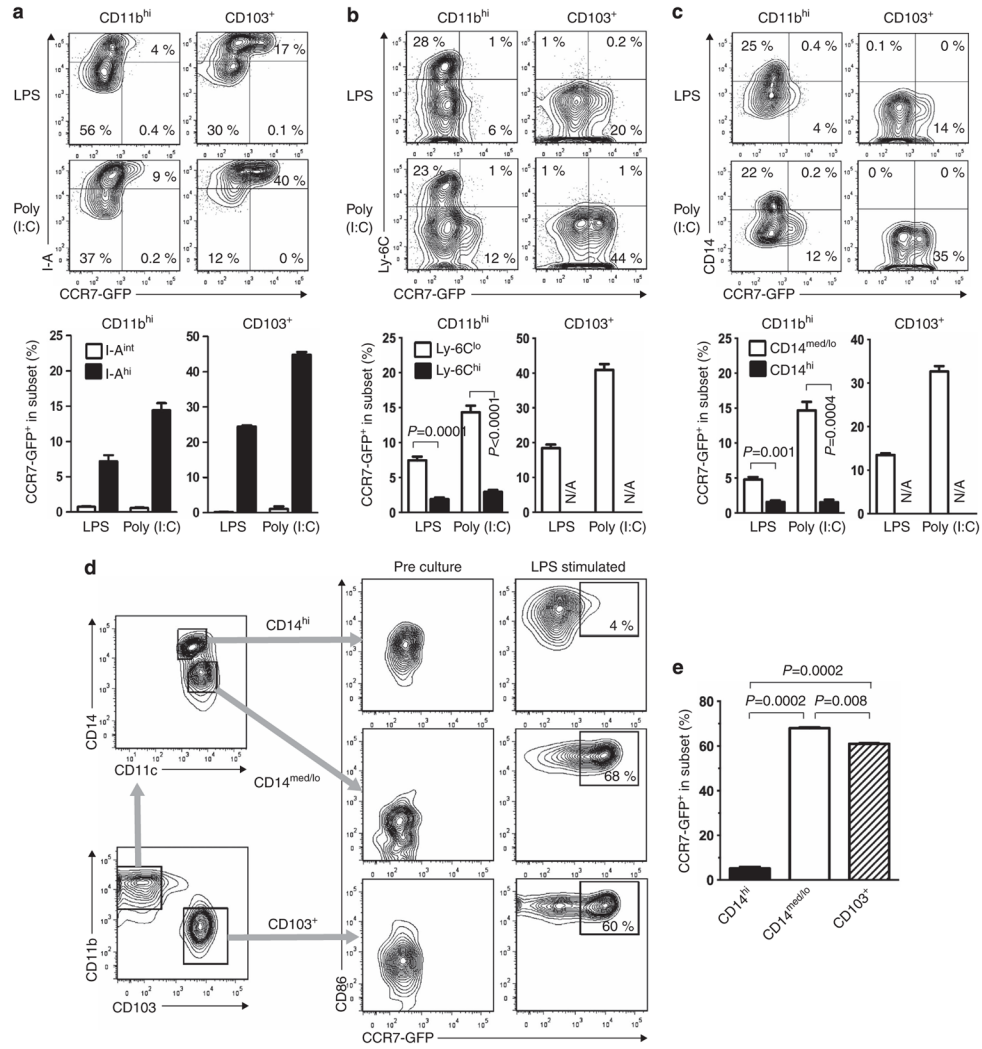


Figure 3. *Ccr7* expression in CD11b^{hi} dendritic cells (DCs) is restricted to Ly-6C^{lo}CD14^{med/lo} DCs. (a–c) Co-production of CCR7-GFP (CCR7-green fluorescent protein) with I-A (a), Ly-6C (b), or CD14 (c) in the indicated pulmonary DC subsets 24 h after instillation of lipopolysaccharide (LPS) or polyinosinic-polycytidylic acid (poly (I:C)). (*n* = 3 mice/group). A representative result of two independent experiments is shown. (d) Gating strategy for purifying CD14^{hi}CD11b^{hi}, CD14^{med/lo}CD11b^{hi}, and CD103⁺ DCs from the lung (left) and expression of CCR7-GFP before and after *ex vivo* culture of the cells in LPS-containing media (right). Levels of CD86 are also shown. (e) Compiled data (*n* = 2/group) of CCR7-GFP expression in the indicated DC subsets following LPS stimulation *ex vivo*. N/A, not applicable.

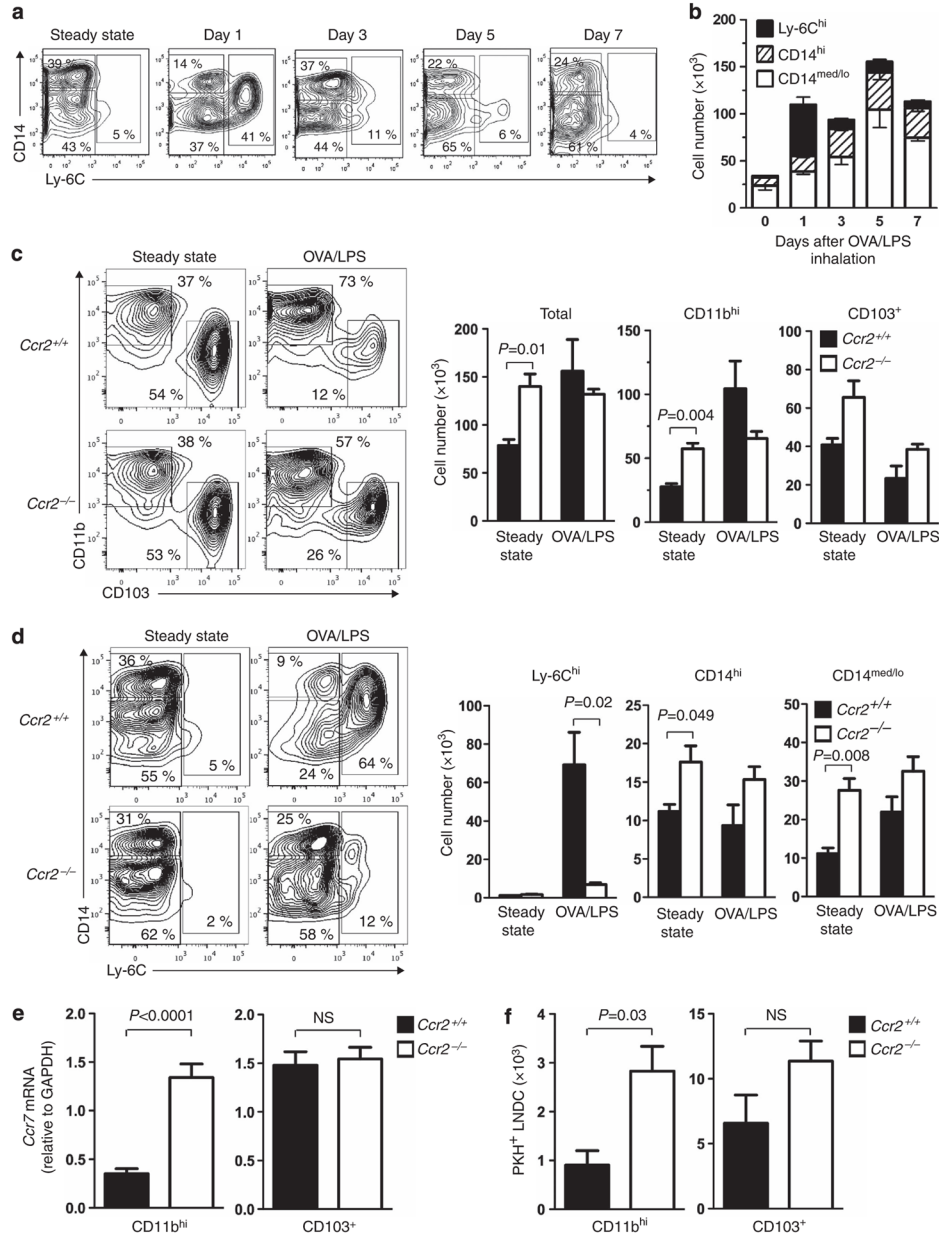
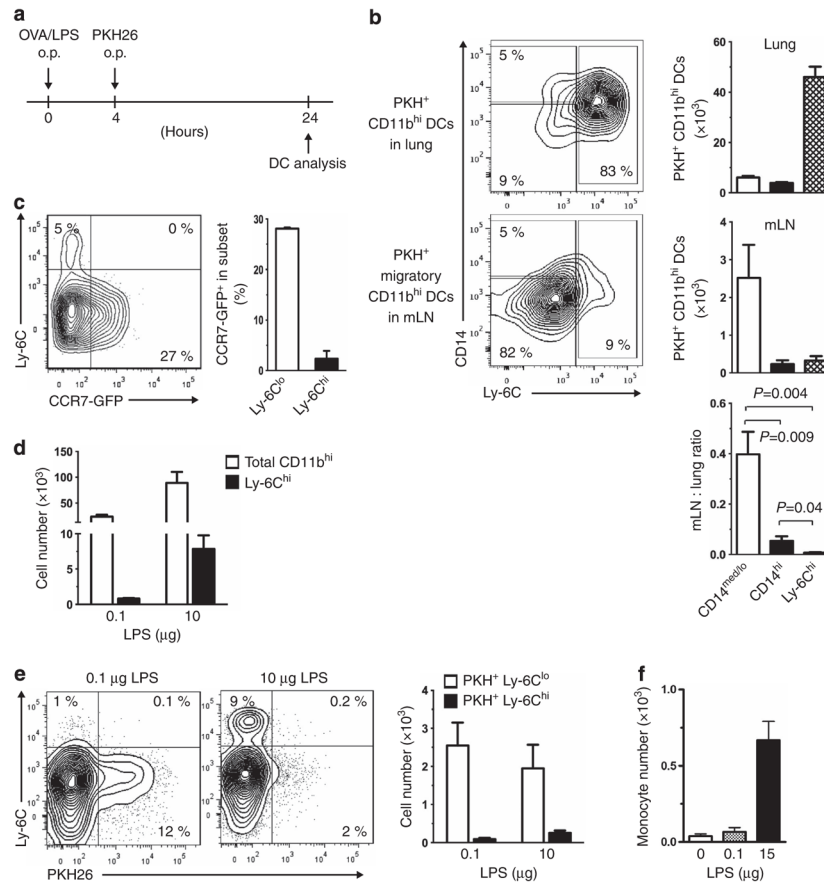


Figure 4.

Analysis of three distinct subpopulations of CD11b^{hi} dendritic cells (DCs) in the lung. **(a)** Cytochrome plots showing CD14 and Ly-6C staining of DCs within a CD11b^{hi}CD11c⁺I-A⁺ gate at the indicated times following ovalbumin/lipopolysaccharide (OVA/LPS) instillation and **(b)** absolute number of cells in each subpopulation. **(c)** Cytochrome plots showing CD103 and CD11b staining of total lung DCs in wild-type and *Ccr2*^{-/-} mice (left). Also shown are numbers of total, CD11b^{hi}, and CD103⁺ lung DCs under steady-state conditions and 16 h after OVA/LPS instillation (right) (*n*=3). **(d)** Cytochrome plots showing CD14 and Ly-6C staining of CD11b^{hi} lung DCs in wild-type and *Ccr2*^{-/-} mice (left). Numbers of Ly-6C^{hi}, CD14^{hi}, and CD14^{med/lo} DCs under steady-state conditions and 16 h after OVA/LPS instillation are shown (right) (*n*=3). **(e)** *Ccr7* mRNA levels in the indicated lung DC subsets of LPS-treated mice (*n*=2 to 7). **(f)** Number of PKH⁺ migratory CD11b^{hi} and CD103⁺ DCs in the

mediastinal lymph nodes (LNs) of wild-type and *Ccr2*^{-/-} mice 24 h after LPS instillation ($n=3$). A representative result of two independent experiments is shown. GAPDH, glyceraldehyde 3-phosphate dehydrogenase; NS, not significant.

**Figure 5.**

Inflammatory dendritic cells (DCs) in the lung do not migrate to mediastinal lymph nodes (mLNs). **(a)** Timeline for instillation of lipopolysaccharide (LPS) and PKH. **(b)** Ly-6C and CD14 display on PKH⁺ CD11b^{hi} DCs from the lung (top) and mLNs (middle). Representative cytograms for individual mice are shown, as well as compiled results for five mice. Also shown is the ratio of the PKH⁺ cells in mLNs and the lung (bottom). **(c)** Expression of *Ccr7-gfp* and staining for Ly-6C on CD11b^{hi} mLN DCs of *Ccr7^{gfp/+}* mice ($n=2$). **(d)** Total and Ly-6C^{hi} CD11b^{hi} inflammatory DCs in mLNs following instillation of either low- (0.1 μg) or high- (10 μg)-dose LPS. **(e)** Ly-6C and PKH staining of CD11b^{hi} DCs in mLNs after LPS instillation. Representative cytograms and compiled results ($n=3$) are shown. **(f)** Accumulation of inflammatory monocytes in mLNs 2 h after intravenous injection of 10⁶ CFSE (carboxyfluorescein diacetate succinimidyl ester)-labeled Ly-6C^{hi}CD11b^{hi} bone marrow cells into recipient mice. Animals were instilled with the indicated amount of LPS 24 h before monocyte transfer ($n=2$). o.p., oropharyngeal; OVA, ovalbumin.

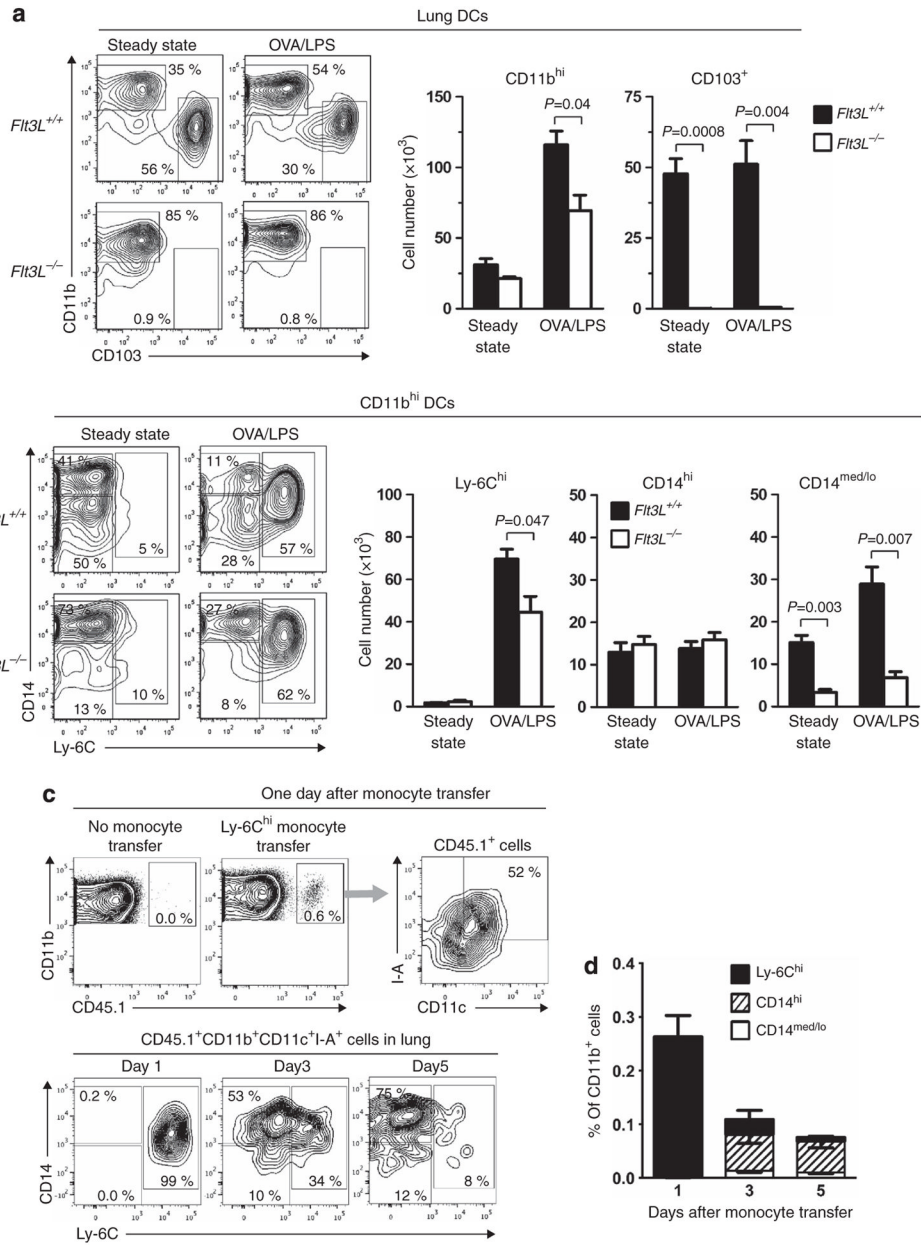
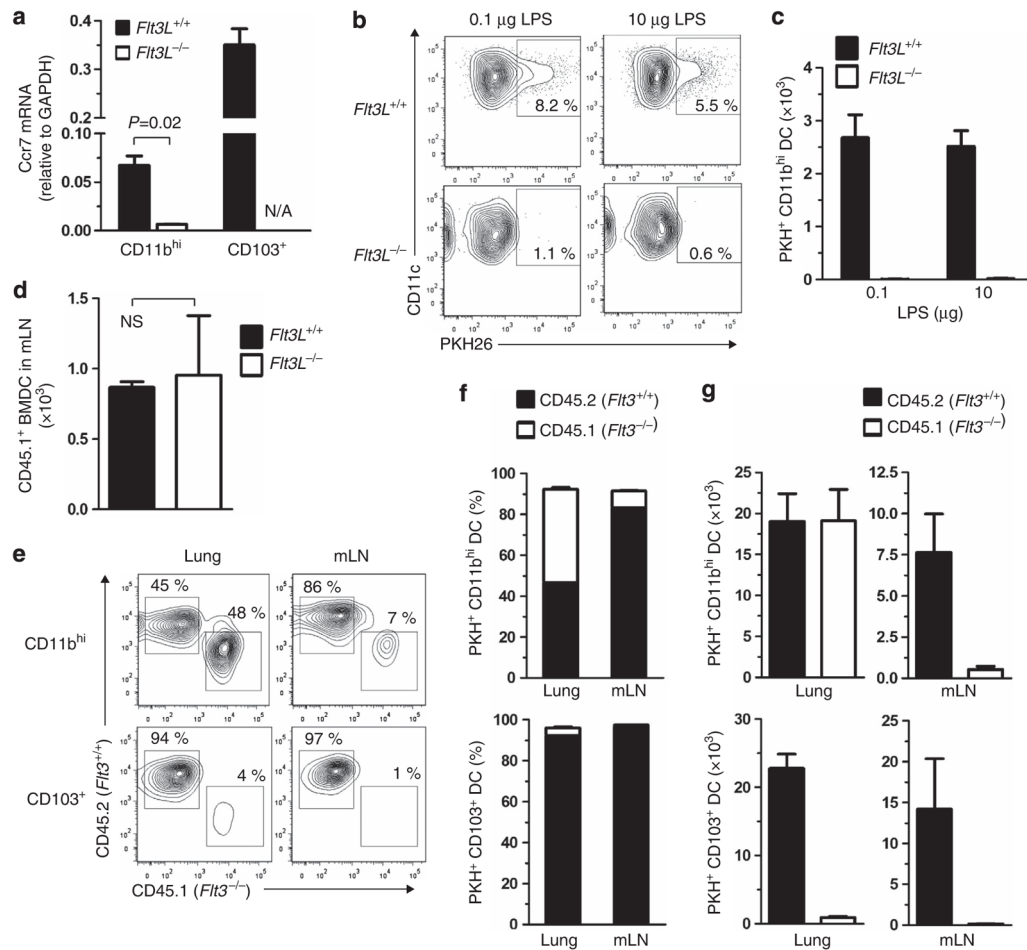


Figure 6. Ly-6C^{hi} and CD14^{hi} cells in CD11b^{hi} dendritic cells (DCs) are monocyte-derived. **(a)** Analysis of major lung DC subsets in wild-type and *Flt3L*^{-/-} mice. Cytochrome plots showing CD103 and CD11b staining of total CD11c⁺I-A⁺ lung DCs (left) and histograms of total, CD11b^{hi}, and CD103⁺ lung DCs under steady-state conditions and 16 h after ovalbumin/lipopolysaccharide (OVA/LPS) instillation (right) (*n*=3). **(b)** Cytochrome plots showing CD14 and Ly-6C staining of CD11b^{hi} lung DCs (left) and histograms of Ly-6C^{hi}, CD14^{hi} and CD14^{med/lo} DCs under steady-state conditions and 16 h after OVA/LPS instillation (right) (*n*=3). **(c)** Cytochrome plots show gating of donor-derived DCs (CD45.1⁺CD11b^{hi}CD11c⁺I-A⁺) (top), and display of CD14 and Ly-6C on those DCs (bottom), following adoptive transfer of CD45.1 Ly-6C^{hi} monocytes (CD3⁻CD11b⁺CD11c⁻CD19⁻CD115⁺I-A⁻Ly-6C⁻TER119⁻7-AAD⁻). Recipient CD45.2 mice were instilled with OVA/LPS 2 hrs prior to the monocyte

transfer. **(d)** Histograms showing the number of monocyte-derived DCs corresponding to the indicated populations ($n=3$). A representative result of three independent experiments is shown.

**Figure 7.**

FLT3L/FLT3L-independent, monocyte-derived CD11b^{hi} dendritic cells (DCs) are non-migratory. (a) *Ccr7* mRNA levels in lung DC subsets of wild-type and *Flt3L*^{-/-} mice as measured by qPCR (*n*=2 to 9). (b, c) PKH⁺ migratory CD11b^{hi} DCs in mediastinal lymph nodes (mLNs) 24 h after lipopolysaccharide (LPS) instillation into airways of wild-type and *Flt3L*^{-/-} mice (*n*=3). A representative result of two independent experiments is shown. (d) Migration of wild-type (CD45.1) bone marrow-derived DCs (BMDCs) to mLNs in wild-type and *Flt3L*^{-/-} mice (both CD45.2) following airway instillation of the donor DCs followed by ovalbumin/LPS 4 h later. Analysis of mLNs from recipient mice was performed 20 h later by flow cytometry. (e–g) Migration assay of *Flt3L*^{-/-} DCs from lung to mLNs. (e) Mixed BM chimeric mice were generated by transfer of a mixture of wild-type (CD45.2) and *Flt3L*^{-/-} (CD45.1) BM cells into irradiated wild-type (CD45.2) mice. Lung and mLN DCs in the recipients were analyzed 16 h after PKH instillation to airway. Flow plots of cells displaying CD45.1 or CD45.2 in PKH-gated CD11b^{hi} and CD103⁺ DCs are shown. Percentage (f) and absolute number (g) of PKH⁺ wild-type and *Flt3L*^{-/-} DCs in lung and mLNs of the chimeric mice. A representative result of two independent experiments is shown. GAPDH, glyceraldehyde 3-phosphate dehydrogenase; N/A, not applicable; NS, not significant.